

Cluster winds blow along supercluster axes

Dmitri I. Novikov,¹ Adrian L. Melott,¹ Brian C. Wilhite,¹ Michael Kaufman,¹
Jack O. Burns,² Christopher J. Miller³ and David J. Batuski³

¹*Department of Physics and Astronomy, University of Kansas, Lawrence, Kansas 66045, USA*

²*Office of Research and Department of Physics and Astronomy, University of Missouri, Columbia, Missouri 65211, USA*

³*Department of Physics and Astronomy, University of Maine, Orono, Maine 04469-5709, USA*

Accepted 1998 December 30. Received 1998 December 30; in original form 1998 August 7

ABSTRACT

Within Abell galaxy clusters containing wide-angle tailed (WAT) radio sources, there is evidence of a ‘prevailing wind’ which directs the WAT jets. We study the alignment of WAT jets and nearby clusters to test the idea that this wind may be a fossil of drainage along large-scale supercluster axes. We also test this idea with a study of the alignment of WAT jets and supercluster axes. Statistical tests indicate no alignment of WAT jets towards nearest neighbour clusters, but do indicate approximately 98 per cent confidence in alignment with the long axis of the supercluster in which the cluster lies. We find a preferred scale for such superclusters of order $25 h^{-1}$ Mpc.

Key words: galaxies: clusters: general – intergalactic medium – large-scale structure of Universe.

1 INTRODUCTION

Galaxy clusters are often elongated. Binggeli’s (1982) study of Abell cluster data gave the first indication that they have a strong tendency towards alignment with (i.e. their semimajor axes point toward) other clusters at distances of less than around $30 h^{-1}$ Mpc. West’s (1989) study of 48 superclusters also gave clear evidence for alignment of clusters within superclusters on similar scales. Simulations also indicate that cluster axes are aligned with neighbouring clusters (Splinter et al. 1997, and references therein).

It has become recognized within the context of structure formation in hierarchical clustering (‘bottom-up’) owing to gravitational instability that the large-scale weakly non-linear structure closely follows that produced in what used to be called the ‘top-down’ or ‘pancake’ theory (Melott et al. 1983; Pauls & Melott 1995, and references therein; Bond, Kofman & Pogosyan 1996). In this picture, most galaxy clusters are formed by the flow of matter along the sheets and filaments that connect neighbouring clusters (Shandarin & Klypin 1984; Colberg et al. 1999).

For this reason, merging events are often aligned with these structures. Mergers inject a velocity anisotropy into the cluster that should persist for several crossing times. It may be a cause for the tendency of clusters to point to their neighbours as described above. The anisotropy is a fossil relic of recent merging events, which can be seen most clearly in the simulation video (particularly the second sequence) accompanying Kauffmann & Melott (1992).

Burns (1998) has reviewed the evidence for persistent winds in the intracluster medium that may exist as a result of these recent mergers (see also Roettinger, Burns & Loken 1996 and Gomez et al. 1997a). Gomez et al. (1997b) showed that there is a highly

significant correlation between the orientation of the semimajor axis of the cluster and the direction of these winds, as indicated by the bending of jets from wide-angle tailed (WAT) radio sources in the clusters. On the other hand, Ulmer, McMillan & Kowalski (1989) found no orientation of X-ray images toward nearest neighbour clusters.

Although there is evidence of alignment between cluster ellipticity and neighbouring clusters, and of alignment of cluster ellipticity with the winds blowing WAT jets, there has been no study of the alignment of WAT jets with neighbouring clusters. It is possible that the ‘prevailing wind’ seen in Abell clusters with WATs may be a remnant of drainage along large-scale structure. If this wind is a fossil of such drainage, one might expect that it will point either to neighbouring clusters or along supercluster axes.

2 PROCEDURE

Images from O’Dea & Owen (1985), Zhao, Burns & Owen (1989), O’Donoghue, Eilek & Owen (1990), Pinkney et al. (1993) and Gomez et al. (1997b) have been used in the determination of the orientation of WAT radio source jets. These images are overlays of 6- or 20-cm Very Large Array (VLA) data on X-ray emission contours in the 0.5–2.0 keV energy band from *ROSAT* Position Sensitive Proportional Counter (PSPC) data. Another image used is of data from the Westerbork radio telescope at 6 cm (Vallee, Wilson & VanDerLaan (1979). To estimate the direction of the ‘wind’ within a cluster, lines are drawn manually upon the WAT jets, and a bisector drawn for the angle created by these lines. Since the clusters are all at a large distance from Earth, a small-angle approximation is used. The orientation of each bisector in Table 1

Table 1. Estimated orientation angles for winds in the WAT clusters studied. Note that all angles are taken with respect to the horizontal and are in degrees. Uncertainties represent one standard deviation from estimates by five individuals.

| Cluster | WAT orientation | Uncertainty |
|---------|-----------------|-------------|
| A400 | 124.3 | 6.0 |
| A562 | 320.2 | 0.2 |
| A690 | 57.6 | 2.4 |
| A1446 | 215.0 | 7.6 |
| A1569 | 203.8 | 2.0 |
| A1656 | 44.6 | 3.5 |
| A1940 | 328.6 | 1.4 |
| A2214 | 248.3 | 9.1 |
| A2304 | 357.9 | 4.2 |
| A2306 | 292.5 | 1.7 |
| A2462 | 288.1 | 1.1 |
| A2634 | 307.6 | 2.8 |

is reported with respect to the horizontal. An orientation of 0° or 360° corresponds to a cluster with a WAT that ‘points’ to the east on a flattened section of celestial sphere. To reduce the effect of subjectivity upon the estimated orientation of the WATs, lines are constructed independently by five different individuals with no knowledge of the environment of the cluster. As can be seen in Table 1, the random uncertainties in the WAT angle estimation are relatively small and will have little effect on questions of alignment.

We have not considered sources for which orientations were difficult to ascertain for any reason (e.g. extreme ambiguity of orientation; difficulty in determining location of one of the WAT jets; poor spatial radio resolution of the more distant WATs; no apparent wind as evidenced by an opening angle near 180°). We have also excluded WATs that live in clusters for which no neighbours exist in our redshift catalogue within $30h^{-1}$ Mpc, where $h = H_0/100 \text{ km s}^{-1} \text{ Mpc}^{-1}$. (This is sometimes due to lack of redshift information.) This leaves us with 12 of the 17 different WATs that were present in our source studies.

Owing to the redshift survey incompleteness, it is not possible to define a complete sample of clusters for the WATs in this analysis. However, given these constraints, we believe that the remaining sample of WAT clusters and their neighbours is not systematically biased and should be representative of such clusters and their environs.

For each of the 12 WATs, we first search the Abell cluster catalogue to find the nearest neighbour cluster. Although all WAT angle bisectors are drawn against a flattened celestial sphere, we find neighbour clusters in three-space. The cluster neighbours of each WAT source are determined using Abell clusters of all richness and distance classes north of -27° declination. In most cases, only clusters with measured redshifts are used. However, approximately 15–20 per cent of Abell clusters with $m_{10} \leq 17.0$ do not as yet have measured redshifts, so occasionally the Batuski & Burns (1985) $m_{10}-z$ relation is used. The data for the clusters with observed redshifts come from a variety of sources including Struble & Rood (1987) and Postman, Huchra & Geller (1992). However, the majority of the cluster redshifts with $m_{10} \geq 16.5$ and $R \geq 1$ have been supplied by the MX Survey and its extension (Slinglend et al. 1998; Miller et al., in preparation). The MX Survey was designed to measure all $R \geq 1$ Abell clusters with $m_{10} \leq 17.0$ in the Northern Hemisphere. Currently, the sample of $R \geq 1$, $0^h \leq \alpha \leq 24^h$,

Table 2. The nearest neighbour cluster and the angle between WAT orientation and a line connecting the WAT and nearest neighbour for each of the clusters studied.

| WAT Cluster | Nearest neighbour | Angle (degrees) |
|-------------|-------------------|-----------------|
| A400 | A397 | 36.0 |
| A562 | A556 | 3.3 |
| A690 | A699 | 17.6 |
| A1446 | A1402 | 22.5 |
| A1569 | A1526 | 70.3 |
| A1656 | A1367 | 62.9 |
| A1940 | A1936 | 37.0 |
| A2214 | A2213 | 14.0 |
| A2304 | A2304 | 65.5 |
| A2306 | A2305 | 69.9 |
| A2462 | A2459 | 82.2 |
| A2634 | A2666 | 50.3 |

$-17^\circ \leq \delta \leq 90^\circ$ (1950) and $|b| \geq 30^\circ$ Abell clusters is 87 per cent complete to $m_{10} = 17.0$, with 282 out of 324 having measured redshifts. When the $R = 0$ clusters are included, the sample is 80 per cent complete with 457 out of 569 clusters having measured redshifts. About 90 per cent of the clusters that we use have measured redshifts. Two of the nearest neighbours (for A562 and for A2306) have estimated redshifts, but dropping these would not modify our conclusions about nearest neighbours described in the next section. The remaining estimated redshifts are merely a source of foreground/background noise, since we study projected alignments.

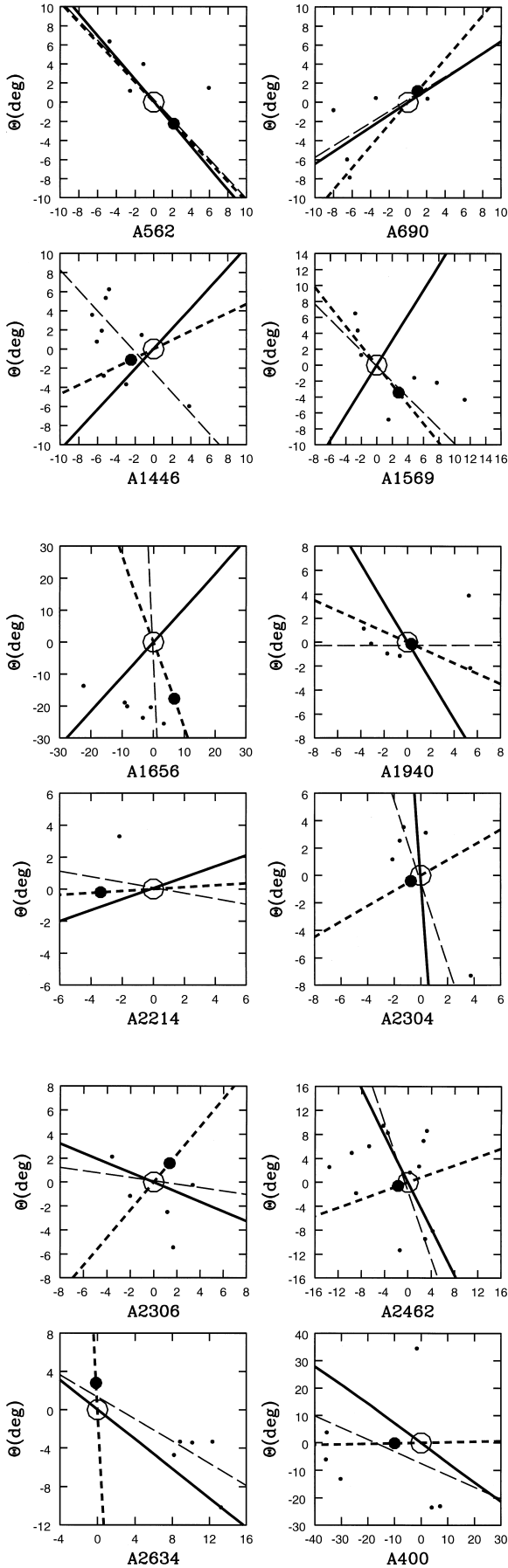
All calculations in this paper are made using lines projected upon the celestial sphere and then flattened owing to the assumption of a small-angle approximation. These calculations should be valid, however, since all these cluster neighbourhoods pictured are relatively small. The largest angular separation between WATs and included clusters is approximately 25° .

When the nearest neighbour is determined, a line is constructed which connects the WAT cluster to the nearest neighbour. The angle ϕ_i between this line and the WAT bisector is recorded for each of the clusters in Table 2 (index i denotes the number of the WAT). Fig. 1 shows the cluster environments and the various orientations that we compare. The distribution of these angles is under consideration. We also have available an image which can be found at <http://kusmos.phsx.ukans.edu/images/A2634SUW.jpg>, which shows the cluster gas in an X-ray false colour image (Burns et al. 1994), the jets from VLA data, and the cluster oriented in its supercluster environment.

If there is no correlation between the orientations of WATs and the directions of the lines connecting WATs and their neighbours, the angle ϕ between them should be uniformly distributed from 0° to 90° and have a mean angle

$$\bar{\phi} = \frac{1}{N} \sum_{i=1}^N \phi_i = 45^\circ, \quad (1)$$

where N is the total number of WATs. If there were any alignment between WAT bisectors and nearest neighbour clusters, then $\bar{\phi}$ would obviously be less than 45° . Equation (1) is accurate for large N , but we have only 12 WATs. $\bar{\phi}$ is 44.4 , and a Kolmogorov–Smirnov test shows no significant evidence that the distribution is non-uniform (see the next section).



We also check for WAT alignment with the supercluster in which the cluster lies. We again search the Abell catalogue, this time to locate clusters within $50 h^{-1}$ Mpc of each WAT cluster. We loosely call such a set of clusters (including the WAT and nearest neighbour clusters) a ‘supercluster’. We do not include clusters at larger distances from the WAT because this typically forces part of the volume into galactic obscuration or out of the survey region. We have simulated the effect of additional neighbours distributed randomly with the global sample mean density out to $100 h^{-1}$ Mpc and find that, while it adds some extra noise, it does not remove our alignment signal.

We next determine the orientation of the supercluster long axis. We wish to fit a straight line to the collection of clusters by drawing a least-squares line based on the projection of each cluster on the flattened celestial sphere. We need to include clusters within a finite distance, to take account of the fact that nearby clusters are more likely to lie within the same structure as the WAT. However, we would like to avoid sudden changes in orientation as this limit is changed to include a new cluster. We therefore apply a least-squares fit to a straight line, but clusters are Gaussian-weighted, $\exp(-r^2/2r_0^2)$, for proximity to the WAT cluster. An advantage of this approach is that we can explore the effect of changes in r_0 . The angles between the WAT bisectors and these lines are calculated and recorded in Table 3. We have used bootstrap resampling (Barrow, Bhavsar & Sonoda 1984) to estimate the uncertainty in the angles. For our small number of clusters this procedure is likely to overestimate the uncertainties, so these can be regarded as upper limits to 1σ uncertainties. It is also true that our result does not depend on the assumption that the superclusters are straight lines, while these are the uncertainties in a fit to a straight line, but it is the best that we can do to associate some kind of error bars with the orientation of

Table 3. The angle between the WAT jet bisector and the line defining the orientation of the supercluster for each of the WAT clusters studied. The supercluster orientation is that for $r_0 = 21 h^{-1}$ Mpc (see text).

| WAT cluster | WAT–supercluster angle (degrees) | Uncertainty (degrees) |
|-------------|----------------------------------|-----------------------|
| A400 | 11.0 | 24.1 |
| A562 | 3.5 | 13.2 |
| A690 | 0.4 | 8.7 |
| A1446 | 86.2 | 7.6 |
| A1569 | 77.1 | 10.8 |
| A1656 | 45.6 | 7.6 |
| A1940 | 59.6 | 8.5 |
| A2214 | 27.0 | 23.0 |
| A2304 | 14.8 | 14.6 |
| A2306 | 12.4 | 25.1 |
| A2462 | 6.3 | 12.2 |
| A2634 | 6.8 | 7.3 |

Figure 1. In each panel, the open circle denotes the WAT cluster; the solid line shows the orientation of the wind blowing the WAT jets; the short-dashed line connects the WAT cluster with the nearest neighbour cluster (the large filled circle); the remaining points show clusters within $50 h^{-1}$ Mpc of the WAT cluster; and the long-dashed line denotes the orientation of the supercluster as described in the text. It must be emphasized that these figures are in projection, while the fit is weighted by the full three-dimensional redshift-space distances between clusters. Thus the line may not *appear* to be a good fit to the distribution of points.

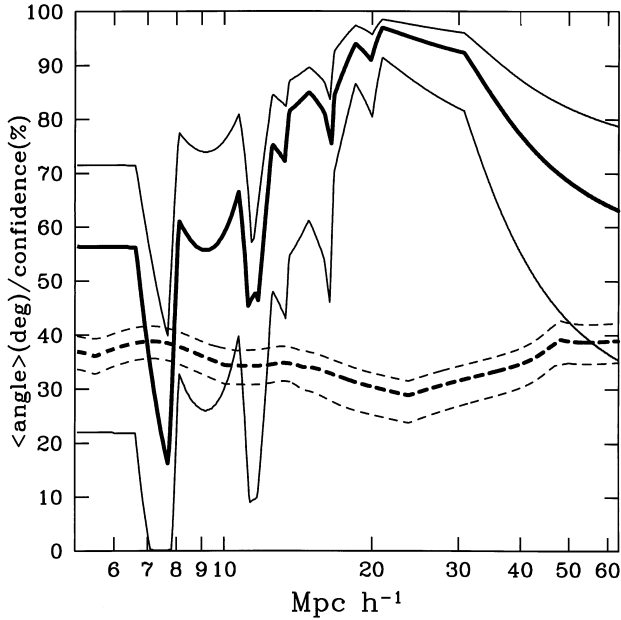


Figure 2. A summary of the results of the supercluster–WAT orientation study. Results are plotted as a function of r_0 , the Gaussian smoothing length for weighting to determine the supercluster orientation. A larger r_0 corresponds to consideration of a larger neighbourhood of the WAT. The heavy dashed line is the mean angle $\bar{\phi}$ between the wind and the supercluster axis. The lighter dashed lines are the same mean computed using the 11 best and 11 worst alignments. The heavy solid line is the confidence level (as computed by a K–S test) that the distribution of angles in the parent population is not uniform. The light solid lines are the same confidence drawn from the 11 best and worst as described above. It is clear that, for superclusters defined in this way, there is a strong tendency for the winds to be aligned with the surrounding region on a scale of about $25 h^{-1}$ Mpc.

the supercluster. The significance of a correlation between the orientation of WAT sources and the supercluster axes can be estimated by investigation of the distribution of these angles in the same way as for nearest neighbours.

Fig. 1 shows the clusters in the vicinity of the named (WAT-bearing) cluster, along with the orientations of the putative wind (WAT bisector), the direction to the nearest neighbour cluster, and the axis fit as described above. It is important that, although actual distances in redshift space are used to decide the weighting, these figures are seen in projection. Since no radial component of the WAT plasma motion is known, we can only look for correlation in the projected angles. Our weighting is based on three-dimensional distances, but the pictures are in projection, so the orientation line may not *appear* to be a good fit to the positions of the clusters.

3 RESULTS AND DISCUSSION

We perform two Kolmogorov–Smirnov (K–S) tests (see Fig. 3). The first is done on our distribution of angles between the WAT angle bisector and the line connecting the WAT cluster to its nearest neighbour. This test indicates only a 1.6 per cent confidence level that we may reject the hypothesis of uniform angle distribution. One may ask if cluster wind directions and nearest neighbour directions are correlated with cluster axes, and why they are not correlated with one another. It is not required, but we would like a physical explanation. We speculate that cluster axes are affected by both tidal forces and merger events. One would expect the nearest cluster to dominate the

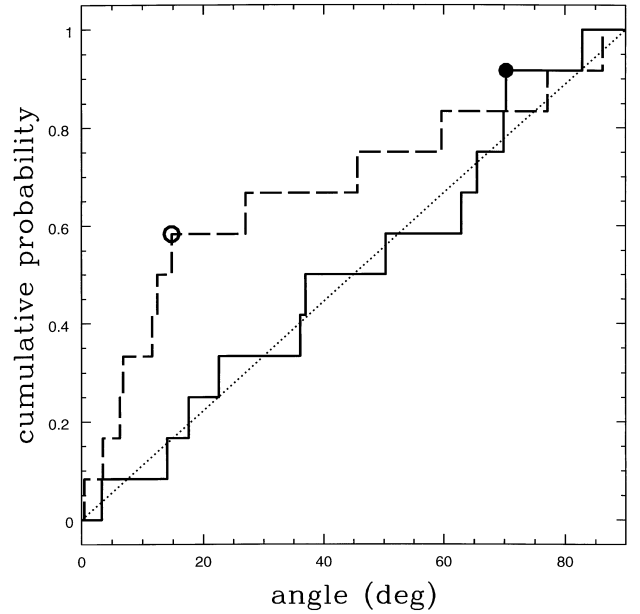


Figure 3. A graphical representation of the K–S tests performed. The dotted diagonal line represents the expected relationship between angle measures and cumulative probability. The solid stair-step pattern represents this relationship within the nearest neighbour distribution of angles. The dashed stair-step pattern corresponds to this same relationship for the distribution of supercluster angles. The larger the maximum deviation of the stair-step pattern from the expected diagonal line, the higher the confidence with which one can reject the hypothesis of a uniform distribution of angles.

tidal field, but merger events should be correlated with the supercluster axis. Further study is needed to understand this null result.

The second test is on the distribution of angles between the wind (WAT angle bisector) and the supercluster line as defined previously. The angle and therefore the significance of its distribution are obviously functions of r_0 . In Fig. 2, the heavy solid line shows the confidence level (for rejection of the null hypothesis that the angles may be distributed uniformly) as a function of r_0 . This confidence reaches a maximum of 97.0 per cent for $r_0 = 21 h^{-1}$ Mpc. The lighter solid lines are a measure of the uncertainty in this confidence, generated by choosing 11 best or 11 worst aligned out of the 12 regions. There is clearly a preferred scale, about $25 h^{-1}$ Mpc. The heavy dashed line is $\bar{\phi}$, which reaches a value of about $29^\circ.3$, when the K–S test reaches maximum confidence. (This is not quite the minimum, which is $28^\circ.8$.) The mean never exceeds 45° , although the confidence is poor for small and large r_0 . Discontinuities in the slope of the confidence curve occur when the slowly rotating supercluster orientations cross 0° or 90° .

For small r_0 , the supercluster orientation is poorly determined, owing to the small number of objects included. As r_0 approaches zero, this becomes the nearest neighbour test. For large r_0 , we exceed the scale of typical segments of the network. It is interesting that the region of best r_0 coincides with the wavelength of perturbations going non-linear today as estimated elsewhere (Melott & Shandarin 1993). It is also close to the neighbour linkage radius found necessary for percolation in one supercluster study (Batuski et al. 1999). We see here support for the idea that the structures found by percolation have a dynamical origin, and are not merely accidental artefacts.

The first K–S test result is consistent with the WAT orientations being completely uncorrelated with nearest neighbours. However, the second K–S test result indicates a strong correlation between WAT wind orientation and the supercluster orientation. It should be noted that a sample size of 12 WAT clusters is very small. West (1989), for example, studied 48 clusters. We recommend investigation of a larger data sample. This will be a lengthy process, dealing with a large number of unclassified sources in the literature.

However, we believe that our conclusions on the supercluster–WAT alignment are robust, and offer several reasons for this. First, the K–S test is useful under certain conditions for small sample sizes. It is statistically robust at the sample size and confidence level of our result (Lehmann & D’Abrera 1975).

Another approach is to use a completely different statistic. If we put the angles into four bins of 22.5° , each of which would be equiprobable under a uniform population, we can use the binomial theorem to evaluate the probability that seven or more out of 12 will lie in the first bin. The result is 98.9 per cent confidence that the distribution is not uniform. Using three bins of 30° produces a similar result (98.5 per cent). Apparently the effect we have found is so strong that it is significant even for a small sample size.

Our results show a correlation between objects two orders of magnitude apart in size. They also provide dynamical evidence in favour of quasi-linear hierarchical clustering following ‘pancake’ dynamics (Melott & Shandarin 1993). This has had great success in reproducing large structure in N -body simulations. It predicted the supercluster–void picture of large-scale structure accepted today (Zel’dovich, Einasto & Shandarin 1982; Melott et al. 1983). However, this general agreement between theory and observation has been based on statistical measures of the galaxy distribution, not on observed dynamics. Analysis of cosmic flows has not yet progressed to showing features unique to the quasi-linear regime. The flows indicated here are not a part of linear theory, and thus lend empirical support to the quasi-linear analysis of gravitational instability.

ACKNOWLEDGMENTS

We are grateful to the referee, M. West, and also to S. Bhavsar for helpful comments and conversations. DIN was supported by an NSF–NATO Fellowship, and other authors at the University of Kansas were supported by the NSF–EPSCoR programme. JOB was supported by the NSF. CJM was funded in part by the

NASA–EPSCoR programme through the Maine Science and Technology Foundation.

REFERENCES

- Barrow J. D., Bhavsar S. P., Sonoda D. H., 1984, *MNRAS*, 210, 19p
 Batuski D. J., Burns J. O., 1985, *ApJ*, 299, 5
 Batuski D. J., Miller C., Slinglend K., Balkowski C., Maurogordato S., Cayatte V., Felenbok P., Olowin R., 1999, *ApJ*, in press
 Binggeli B., 1982, *A&A*, 107, 338
 Bond J. R., Kofman L., Pogosyan D., 1996, *Nat*, 380, 603
 Burns J. O., 1998, *Sci*, 280, 400
 Burns J., Roettiger K., Pinkney J., Loken C., Doe S., Voges W., White R., 1994, in Schlegel E. M., Petre R., eds, *AIP Conf. Proc.* 313, *ROSAT Sci. Symp. on The Soft X-ray Cosmos*. Am. Inst. Phys., New York, p. 183
 Colberg J. M., White S. D. M., Jenkins A., Pearce F. R., 1999, *MNRAS*, submitted (astro-ph/9711040)
 Gomez P. L., Ledlow M. J., Burns J. O., Pinkney J., Hill J. M., 1997a, *AJ*, 114, 1171
 Gomez P. L., Pinkney J., Burns J. O., Wang Q., Owen F. N., Voges W., 1997b, *ApJ*, 474, 580
 Kauffmann G. A. M., Melott A. L., 1992, *ApJ*, 393, 415
 Lehmann E. L., D’Abrera H. J. M., 1975, *Nonparametrics*. Holden-Day, San Francisco, p. 38
 Melott A. L., Shandarin S. F., 1993, *ApJ*, 410, 469
 Melott A. L., Einasto J., Saar E., Suisalu I., Klypin A., Shandarin S., 1983, *Phys. Rev. Lett.*, 51, 935
 O’Dea C. P., Owen F. N., 1985, *AJ*, 90, 927
 O’Donoghue A., Eilek J., Owen F. N., 1990, *ApJS*, 72, 75
 Pauls J., Melott A. L., 1995, *MNRAS*, 274, 99
 Pinkney J., Rhee G., Burns J. O., Hill J. M., Oegerle W., Batuski D., Hintzen P., 1993, *ApJ*, 416, 36
 Postman M., Huchra J. P., Geller M. J., 1992, *ApJ*, 384, 404
 Roettiger K., Burns J. O., Loken C., 1996, *ApJ*, 473, 651
 Shandarin S. F., Klypin A. A., 1984, *SvA*, 28, 491
 Slinglend K. A., Batuski D. J., Miller C. M., Haase S., Michaud K., Hill J. M., 1998, *ApJS*, 115, 1
 Splinter R. J., Melott A. L., Linn A. M., Buck C., Tinker J., 1997, *ApJ*, 479, 632
 Struble M. F., Rood H. J., 1987, *ApJS*, 63, 543
 Ulmer M. P., McMillan S. L. W., Kowalski M. P., 1989, *ApJ*, 338, 711
 Vallee J. P., Wilson A. S., VanDerLaan H., 1979, *A&A*, 77, 183
 West M. J., 1989, *ApJ*, 347, 610
 Zhao J., Burns J. O., Owen F. N., 1989, *AJ*, 98, 64
 Zel’dovich Ya. B., Einasto J., Shandarin S. F., 1982, *Nat*, 300, 407

This paper has been typeset from a \TeX/L\AA\TeX file prepared by the author.